Proceedings of the 2022 International Symposium on Flexible Automation
ISFA2022
July 3 - 7, 2022, Yokohama, Japan

ISFA2022-013

NOVEL DECONVOLUTION BASED FEEDRATE SCHEDULING TOWARDS A NEW CLASS OF CAM FOR TIME-DEPENDENT PROCESSES

Shuntaro Yamato[1]
Dept. of Micro Engineering, Kyoto University
Kyoto, Japan

Burak Sencer
Dept. of Mechanical Engineering, Oregon State University
Corvallis, USA

Anthony Beaucamp
Dept. of Micro Engineering, Kyoto University
Kyoto, Japan

ABSTRACT

Conventional mechanical machining processes such as milling, turning, and grinding are position-dependent processes where the volume of material removed is solely dependent on the engagement geometry of the tool and workpiece. However, advanced precision polishing processes with a compliant tool, fluid jet, or laser are characterized as time-dependent processes (TDP) where the volume of material removed depends not only on the tool position but also on its influence duration on the workpiece. Accordingly, accurate planning of the feedrate profile in sync with the tool position becomes necessary to accurately control the material removal rate and final target shape profile. A novel feedrate planning algorithm is proposed in this paper, which schedules the position-dependent feedrate based on the time-dependent process dynamics and the target shape profile. The feedrate profile is designed as a B-spline, and control points are optimized in the sense of least squares based on the process dynamics and target final shape. The developed algorithms were demonstrated in fluid jet polishing of precision optics.

Keywords: Feed scheduling; Fluid jet polishing; Inverse dynamics.

NOMENCLATURE

α, β, γ	Parameters of Gaussian function
B^n	n-th degree of B-spline basis function
d	Control point
F	Feedrate
G^n	n-th degree of material removal basis function
H	3-dimensional tool influence function
$\bar{H}$	Dimensionally reduced tool influence function
N_c	Number of control points
p	Path spacing
R	Radius of tool influence function
VRR	Volumetric removal rate
x, y	Position coordinate regarding workpiece surface
X, Y	Position coordinate regarding FJP nozzle
X_s, X_e	Start and end X positions in the raster path
z	Amount of material removed
z_d	The target amount of material removed

1. INTRODUCTION

In recent years, advanced CNC polishing processes with a compliant tool [1], fluid jet [2], and laser [3] are developed as finishing methods for precision optical lenses, mirrors, and molds. Unlike conventional mechanical machining, these processes are characterized as time-dependent processes (TDP) where the volume of material removed depends not only on the tool position but also on its influence duration on the workpiece. Therefore, planning of feedrate profile in sync with the tool/nozzle position is a quite important task to accurately control the material removal rate and thus final shape profile. For this purpose, a complex inverse problem related to TDP dynamics, and the target shape profile must be solved.

By precedent researchers, several algorithms have been proposed for planning feedrate in TDP such as ion-beam figuring [4] and fluid jet polishing (FJP) [5]. To the authors' knowledge, the most simple feedrate planning in abrasive TDP is a method based on an approximate analytical model where the feedrate F on work surface points (x, y) is calculated by a volumetric

[1] Contact author: yamato@prec.kyoto-u.ac.jp

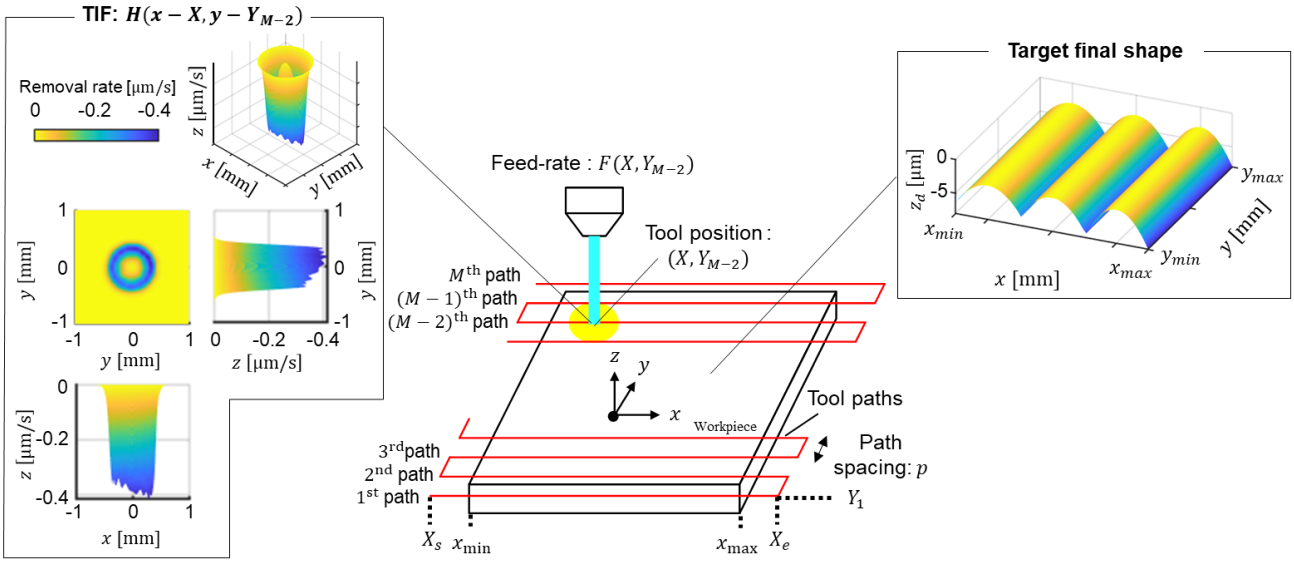

FIGURE 1: SCHEMATIC OF FJP PROCESS WITH RASTER PATHS

removal rate (VRR) of the process, raster-path spacing p, and target amount of material removed z_d as follows [5]:

$$F(x,y) = \frac{VRR(x,y)}{z_d(x,y)p(x,y)} \tag{1}$$

The advantages of this method are exceptionally low computation cost, and the resultant feedrate profile will not be unstable. However, Eq. (1) does not consider the process influence area (i.e., footprint) and regards that the total VRR of the footprint is concentrated at the calculation point (x, y). This indicates that the error of the finished shape will be large if the amount of target removed dynamically changes within the sphere of process footprint, although Eq. (1) is may valid for quasi-static target shapes with gradual undulations.

The feedrate scheduling considering the sphere and its overlap of process footprint can be achieved by solving deconvolution with the discretized process footprint map in each path. To elaborately accomplish deconvolution-based feed-rate scheduling, some algorithms have been also proposed in previous studies [4]. However, conventional deconvolution approaches are typically time-costly and tend to schedule highly variable feed profiles to finely replicate the target geometry. Also, it is challenging to solve deconvolution considering both the feed speed and acceleration constraints at the same time as machine limitations. Therefore, the achievability of the obtained feedrate profile has not been considered.

Accordingly, the purpose of this research is to propose a novel feedrate planning algorithm in which the feedrate profile is designed as a B-spline. To optimize control points, the deconvolution is solved with a newly defined basis function consisting of a B-spline basis function and a process footprint map. The developed algorithms were demonstrated in fluid jet polishing (FJP) of optics glass. In the following section, material removal modeling in FJP is outlined first. Then, the proposed feedrate scheduling method is explained in Section 3 followed by experimental verification in Section 4. Finally, the highlights of this paper are summarized in the conclusion.

2. MODELLING OF MATERIAL REMOVED IN FJP

The material removal in FJP proceeds by the slurry sprayed at high pressure from a nozzle scrapes the workpiece surface. The amount of material removed varies depending on the time duration of the slurry impingement to the workpiece at each path position. Regarding path generation, a simple raster path is often employed for freeform sub-aperture CNC polishing [5]. For its simplicity, this paper also focuses on the raster paths as shown in FIGURE 1. Since the process footprint by fluid jet is spread out from the nozzle center, the amount of material removed at a given location becomes the convolution of the material removal on each raster path. Therefore, the material removed at a certain position $z(x, y)$ can be expressed mathematically as follows:

$$z(x,y) = \sum_{m=1}^{M} \int_{X_s}^{X_e} H(x-X, y-Y_m)\, D(X, Y_m)\, dX \tag{2}$$

where

$$D(X, Y_m) = \frac{1}{F(X, Y_m)} \tag{3}$$

where $H(x-X, y-Y_m)$ and $D(X, Y_m)$ are the process footprint and dwell-time density being reciprocal of feed speed on m-th raster path, respectively. Note that (x, y) and (X, Y) represent the position coordinates regarding workpiece surface and FJP nozzle, respectively.

The process footprint, H, is a removal rate per unit time and is called a *tool influence function* (TIF). The TIF is a function that varies depending on many factors such as the impingement angle, nozzle-workpiece distance, and fluid-jet pressure as well as material, diameter, and concentration of abrasive grain in the slurry. Generally, TIF is expressed as the sum of Gaussian functions like the Gaussian mixture model as [5]:

$$H(x,y) = \begin{cases} \sum_i \alpha_i \exp\left(-\frac{(x-\beta_{x,i})^2}{2\gamma_{x,i}^2} - \frac{(y-\beta_{y,i})^2}{2\gamma_{y,i}^2}\right), & x^2+y^2 \le R^2 \\ 0, & x^2+y^2 > R^2 \end{cases} \tag{4}$$

where n is the number of Gaussian functions, and α_i, $\beta_{j,i}$, and $\gamma_{j,i}$ $(j = x, y)$ are constants being the scale, width, and center of i-th Gaussian function. Here, Eq. (4) is truncated at a finite radius value R, within which the material is removed. A typical example of the TIF shape in the FJP process is embedded also in FIGURE 1.

For further simplification, this paper assumes that the amount of material removed is the same along the pick feed direction in raster paths (i.e., y-direction in FIGURE 1), and consequently, the dwell time density becomes equal along the y-direction: $D(X, Y_m) \rightarrow D(X)$. Note that, however, the proposed method in the following section can be extended for freeform shapes where the target amount of material removed changes in both the feed and pick feed direction. From the above, Eq. (2) can finally be folded into a dimensionally reduced expression as follows:

$$z(x, y) = \int_{X_s}^{X_e} \bar{H}(x - X) D(X)\, dX \tag{5}$$

where

$$\bar{H}(x - X) = \sum_{m \in \{|y - Y_m| \le R\}} H(x - X, y - Y_m) \tag{6}$$

3. FEEDRATE SCHEDULING ALGORITHM

From Eq. (5), the shape of the finished surface is expressed in the form of a convolution between $\bar{H}$ and D. Since the dwell-time density D is simply reciprocal of the feedrate, the feedrate scheduling can be done by inversely solving the discretized Eq. (5) in the sense of linear least squares, which is known as *deconvolution*. Additionally, the limitation of feed speed in a machine can be considered by imposing the maximum and/or minimum constraints on the dwell time density. However, the direct solution of deconvolution in Eq. (5) is usually very time-consuming and costly due to the large matrix size. Also, the resultant scheduled feedrate can often have a noisy profile because the continuity of adjacent dwell time value is not considered. This results in a violent acceleration profile that the machine cannot follow. Nevertheless, it is challenging to directly impose acceleration constraints on the convolution of Eq. (5), because the relationship between dwell time density and acceleration is non-linear in the spatial domain.

To overcome the above problems, a modified deconvolution approach is proposed, in which the feedrate profile is designed as a B-spline as follows:

$$D(X) = \sum_{i=1}^{N_c} B_i^n(X) d_i \tag{7}$$

where B^n represents a basis function of n-th degree of B-spline, and also d and N_c are control point and its number, respectively. By substituting Eq. (7) for Eq. (5), Eq. (5) can be rearranged to the modified convolution form as:

$$z(x) = \sum_{i=1}^{Nc} G_i^n(x) d_i \tag{8}$$

where

$$G_i^n(x) = \int_{X_s}^{X_e} \{\bar{H}(x - X) B_i^n(X)\} dX \tag{9}$$

Here, $G^n(x)$ can be regarded as a newly defined basis function that this paper proposes for the first time and named the *material removal basis function*. Based on Eq. (7)-(9), the control points are optimized in the sense of constrained linear least square as:

$$\begin{aligned} \boldsymbol{d} &= \underset{\boldsymbol{d}}{\operatorname{argmin}} \left\| z_d(x) - \sum_{i=1}^{Nc} G_i^n(x) d_i \right\|_2^2 \\ \text{subject to: } D(X) &= \sum_{i=1}^{N_c} B_i^n(X) d_i \ge \frac{1}{F_{max}} > 0 \end{aligned} \tag{10}$$

Eq. (10) is similar to the conventional deconvolution, and a different point is using the material removal basis function instead of TIF. However, the deconvolution cost in Eq. (10) can significantly decrease because the necessary number of control points is usually much smaller than the full discretized point map of TIF. Additionally, Eq. (10) will be solved considering the continuity of the feed profile according to the degree of B-spline inherently; hence, the obtained feedrate profile will be smoothed. Note that, however, this B-spline smoothing effect and the constraint of maximum feed speed do not guarantee the obtained acceleration is always below the limit. Nevertheless, thanks to knots refinement of the B-spline basis function [6], the acceleration can be constrained. Concretely, the knots closest to acceleration peaks are removed if the obtained acceleration profile is over the limit (see FIGURE 2) and then resolve Eq. (10) with the refined basis functions. In this approach, it may be necessary to solve Eq. (10) several times, but thanks to the reduction of calculation cost, it may not be a large problem. Through that, the number of control points and arrangement of knots can be refined from the initial set considering the achievability of the scheduled feedrate.

4. EXPERIMENTAL VERIFICATION

To verify the proposed method in FJP, a multi-cylindrical lens shape was created on a flat optical glass as shown in FIGURE 1. In the target lens, the width of the shape becomes narrow around the valley of the lined cylindrical lens, which shows the target shapes have high frequency (i.e., low wavelength) components. For such a target shape, the obtained feedrate profile in the conventional deconvolution will not be achievable due to violent speed fluctuation, although the proposed method and Eq. (1) can stably treat it. For comparison, the target lens shape was created with each feedrate scheduled by the proposed method with a cubic B-spline and Eq. (1). For planning feedrate, the TIF was preliminarily found by spot polishing under the same conditions for the lens polish. The experimental conditions are tabulated in TABLE 1

FIGURE 3 shows the average curve of the final shape in the process area, measured by stylus profiling after polishing. As clearly shown in this figure, sharper characteristics around the valley can be achieved by the proposed method, despite the identified TIF diameter spread out to more than 1 mm which is much wider than the valley of the target shape. As

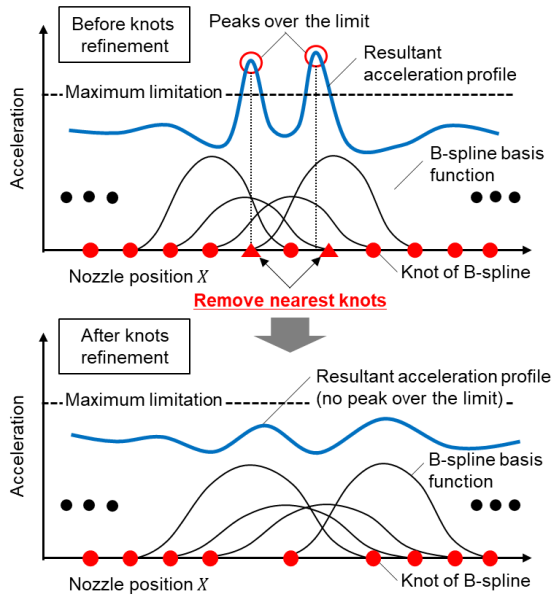

FIGURE 2: ACCLERATION CONSTRAINT THROUGH ITERATIVE KNOTS REFINEMENT

aforementioned in the introduction, the method based on Eq. (1) results in a dull shape because the TIF footprint is not considered. Note that, in both methods, the surface is scraped off more than the target shown in FIGURE 3(a). This was found to be due to a slight DC offset in actual TIF, which did not affect the dynamic components of the obtained shape. Therefore, as is clear from FIGURE 3(b), the proposed method can reproduce the high spatial frequency components of the target finish shape.

5. CONCLUSION

This paper presents a novel deconvolution-based feedrate scheduling with a newly defined material removal basis function that combines the B-spline basis function and the tool influence function. By the proposed method, the calculation cost decreases, and the feedrate scheduling is conducted considering both the feed speed and acceleration limits of a machine in the sense of constrained linear least square and the iterative knots refinement of the B-spline. Through the demonstration of lens shape generation in FJP, the proposed method can reproduce the high spatial frequency components of the target finish shape, which is generally exceedingly difficult to be realized in polishing with the conventional feedrate scheduling method.

ACKNOWLEDGEMENTS

This work was partially supported by JSPS KAKENHI Grant Number 22K14160 and a donation research fund from DMG Mori Seiki Co. The authors acknowledge the support from Zeeko Ltd. in loaning the polishing system and measuring equipment.

REFERENCES

[1] Beaucamp, A., Namba, Y., Combrinck, H., Charlton, P., and Freeman, R., 2014, "Shape Adaptive Grinding of CVD Silicon Carbide," CIRP Ann., **63**(1), pp. 317–320.

TABLE 1: EXPERIMENTAL CONDITIONS

Slurry	$Al_2O_3 + H_2O$
Abrasive size	8.40 ± 0.60 μm
Nominal concentration	20 g/L
Nozzle offset	2 mm
Nozzle diameter	0.5 mm
Impingement angle	90°
Pump pressure	Average 1.27 MPa
Workpiece	N-BK7
Path spacing of raster path	0.06 mm

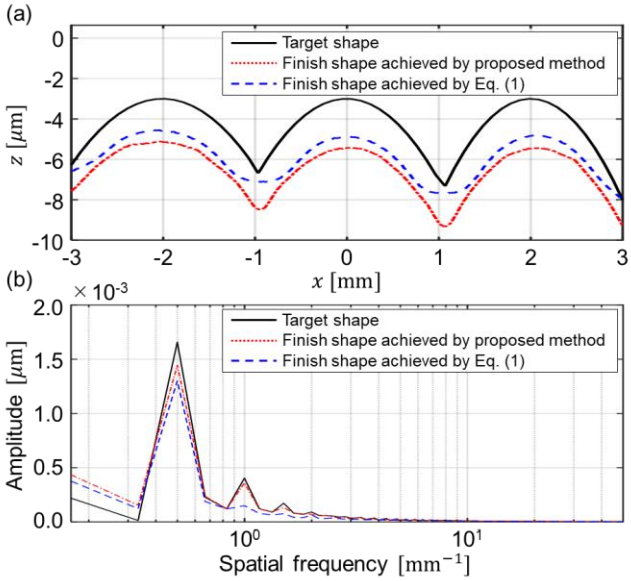

FIGURE 3: FINAL LENS SHAPES: (a) CROSS-SECTION PROFILES, (b) FREQUENCY ANAYSIS OF PROFILE

[2] Axinte, D. A., Karpuschewski, B., Kong, M. C., Beaucamp, A. T., Anwar, S., Miller, D., and Petzel, M., 2014, "High Energy Fluid Jet Machining (HEFJet-Mach): From Scientific and Technological Advances to Niche Industrial Applications," CIRP Ann., **63**(2), pp. 751–771.

[3] Wang, T., Huang, L., Vescovi, M., Kuhne, D., Tayabaly, K., Bouet, N., and Idir, M., 2019, "Study on an Effective One-Dimensional Ion-Beam Figuring Method," Opt. Express, **27**(11), p. 15368.

[4] Wang, T., Huang, L., Kang, H., Choi, H., Kim, D. W., Tayabaly, K., and Idir, M., 2020, "RIFTA: A Robust Iterative Fourier Transform-Based Dwell Time Algorithm for Ultra-Precision Ion Beam Figuring of Synchrotron Mirrors," Sci. Rep., **10**(1), p. 8135.

[5] Han, Y., Zhu, W.-L., Zhang, L., and Beaucamp, A., 2020, "Region Adaptive Scheduling for Time-Dependent Processes with Optimal Use of Machine Dynamics," Int. J. Mach. Tools Manuf., **156**, p. 103589.

[6] Piegl, L., and Tiller, W., 1997, "Curve and Surface Fitting," *The NURBS Book*, Springer Berlin Heidelberg, Berlin, Heidelberg, pp. 361–453.